Deformable Objects Grasping and Shape Detection with Tactile Fingers and Industrial Grippers

Pablo Malvido Fresnillo[a], Saigopal Vasudevan[a], Wael M. Mohammed[a], Jose L. Martinez Lastra[a]
Gianluca Laudante[b], Salvatore Pirozzi[b], Kevin Galassi[c], Gianluca Palli[c]

***Abstract*—In this paper, a cyber-physical system composed by a tactile sensor, a robotic gripper and suitable ROS software nodes is proposed. The tactile sensors are shown to be compatible with three different commercial grippers, and the developed ROS nodes for the data acquisition and elaboration enable the implementation of complex tasks such as the grasping and the shape reconstruction of deformable linear objects like cables. The effectiveness of the systems is tested with cable of different diameters and with wiring harnesses composed by several cables grouped together, focusing on the reconstruction of linear and quadratic curves representing the cable shape. Experimental trials are also executed to show the possibility of exploiting the shape reconstruction provided by the proposed system to correct the gripper grasping pose.**

***Index Terms*—Tactile-Based Grasping, Tactile Sensors, ROS Applications, Deformable Object Manipulation, Cyber-Physical Systems.**

I. Introduction

Deformable objects, such as for example paper, cloths, cables and foods, are extensively manipulated in our everyday life. Thus, deformable object manipulation is an essential skill for robot to enter the human living and working environments. For instance, by obtaining this ability, robots could become more involved in forestry operations [1] or healthcare activities for the elderly and disabled [2]. Moreover, many industrial applications require robots able to manipulate non-rigid objects. Food industry, for example, could boost the production [3], farming industries could use robots to manipulate plants to lessen physical burden on workers [4] and manufacturing industry can minimize labor cost [5]–[7].

However, the manipulation of deformable objects is still a challenging activity for robots. This is the main reason why many assembly procedures involving such deformable objects are still performed manually. One of the main reasons why robots have such limitations in deformable object manipulation is due to the lack of cyber-physical systems including sensing, elaboration and grasping capabilities designed for deformable objects manipulation [8].

[a]FAST-Lab, Faculty of Engineering and Natural Sciences, Tampere University, Tampere, Finland.
[b]Department of Engineering of the University of Campania "Luigi Vanvitelli", Via Roma 29 - 81031, Aversa (CE), Italy.
[c]Department of Electrical, Electronic and Information Engineering "Guglielmo Marconi" (DEI) of the University of Bologna, Italy.
The research leading to these results has received funding from the European Union's Horizon 2020 research and innovation program under grant agreement n° 870133, correspondent to the project entitled REMODEL, Robotic Technologies for the Manipulation of Complex Deformable Linear objects
Corresponding author: *pablo.malvidofresnillo@tuni.fi*

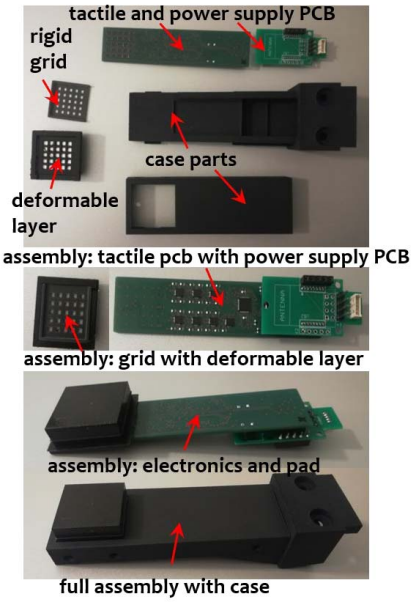

Fig. 1. Detailed view of the sensorized finger.

This paper aims at providing a generic solution for grasping flexible and deformable objects. More precisely, the proposed cyber-physical system is composed by tactile sensors, ROS-based nodes and commercial grippers, and it is purposely designed to grasp Deformable Linear Objects (DLOs) i.e. cables, ropes and hoses. The detection of the position and the shape of DLOs can be performed by exploiting several technologies, such as tactile sensors [9] or machine vision [10], but only the first one can be applied in case of occlusions or manipulation in cluttered scenarios. For this reason, this work focuses on tactile sensing technology in order to provide an integrated solution for deformable objects manipulation, by exploiting and extending the idea proposed in [11]. The main contribution of this paper is testing the performance of this tactile system for the shape reconstruction of different types of cables, in different conditions and orientations, trying to find its limitations, and then, applying this technology for a real cable grasping use case.

The rest of the document is structured as follows. Section II presents the sensing technology and the software components. Section III presents the developed approach for grasping the cable and the experiments to evaluate the grasp correction capabilities. Finally, Section IV reports the conclusions and the possible future work.

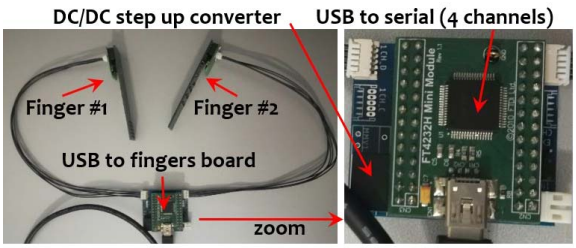

Fig. 2. The electronics for the integration on the gripper.

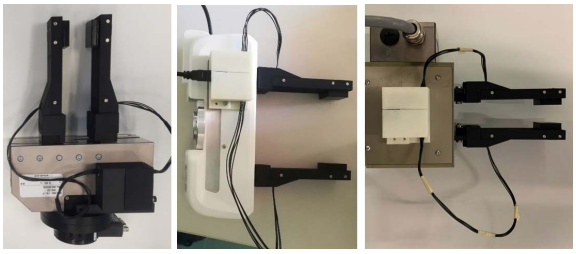

Fig. 3. Example of commercial grippers with integrated sensorized fingers: Schunk WSG-50 (left), Panda gripper (middle) and Schunk PG70 (right).

II. System Description

A. Sensing Technology

Each sensorized finger used in this work is constituted by the following components (shown in top picture of Fig. 1): a tactile Printed Circuit Board (PCB) with the sensing elements, low-level elaboration and conditioning electronics; a second PCB for the microcontroller programming and power-supply; a rigid grid; a deformable layer; a two-part case. The tactile sensors exploited in this paper are based on the working principle originally reported in [12], and continuously improved in various aspects and according to the needs of the applications [9]. The core tactile PCB is constituted by 25 taxels, distributed according to a 5×5 matrix, with a spatial resolution of 3.55 mm both vertically and horizontally. Each sensing point exploits a photo-reflector (manufactured by New Japan Radio, code NJL5908AR) to transduce the local deformation in a voltage variation. The optical components work in reflection mode, i.e., the light emitted by the LEDs is reflected by the white surfaces molded at the bottom side of the deformable layer and measured by the coupled phototransistors integrated in the same device. During a grasping the whole pad deformation is distributively measured in 25 discrete points, by measuring the white surfaces displacements. Differently from previous versions, in this design the LEDs are driven with adjustable current sources to reduce the emitted light drift due to temperature variations. Additionally, analogue buffers have been introduced to decouple the phototransistor voltage signals from the 12−bit A/D channels integrated into the on-board PIC microcontroller. These design choices allowed to simplify the interrogation firmware and to improve the signal-to-noise ratio. The second PCB has been designed in order to allow the programming (and re-programming) of the on-board microcontroller and the serial communication with an external board. The serial communication reaches 500 Hz of sampling frequency for each tactile sensor. Additionally, this PCB allows to manage also the power supplies: an external 24 V for the LED current sources, an external 5 V for the buffers and a 3.3 V (generated on board) for microcontroller and phototransistors.

The design of rigid grid presents protruding edges on three sides, used to mechanically interlock the grid with the PCB edges, for a perfect alignment among taxels and reflective surfaces of the deformable pad. The grid thickness (equal to about 1 mm) has been fixed to guarantee that the photo-reflectors work in a monotonic range. The grid top side presents suitably designed grooves to improve the interlocking robustness among grid and deformable pad. The rigid grid is manufactured in black ABS plastic by using Polyjet 3D printing technology. The deformable pad has the role to transduce the external contacts into deformations that can be detected by the taxels. The flat top side, here presented, allows an easy grasp of wires with the possibility to estimate wire physical features, e.g., shape and diameter. The bottom side present suitable cells with white reflective surfaces in front of the photo-reflectors and black walls to optically separate the taxels. It has been realized in silicone by using suitably molds. The sensorized finger is completed with a two part case: a bottom part designed for the precise housing of the electronic boards; a top part designed to lock the deformable pad along its edges. The case presents at the base two additional holes, different on the basis of commercial gripper in which it is to be integrated. The case is manufactured in nylon by using the Multi Jet Fusion 3D printing technology. The two PCB boards are connected through electronic connectors, while the grid is first assembled with deformable pad by using a cyanoacrylate-based glue (see middle picture in Fig. 1). Then, the assembled mechanical structure (pad with bonded grid) is bonded to the tactile PCB and the resulting sensing system housed in the case, as shown in bottom pictures of Fig. 1.

In order to allow an easy integration of two sensorized fingers in a commercial gripper, an additional PCB, external with respect to the fingers has been designed to drive up to 4 sensorized fingers from a single USB standard port. The core part of the board is constituted by the FTDI chip (FT4232H) which implements a communication port adapter, by allowing to use a standard USB 2.0 port to interrogate up to four TTL serial interfaces with a maximum baud rate of 12 Mbaud for each serial port. Additionally, a step up DC/DC converter has been integrated in order to achieve the 24 V voltage supply needed for LEDs from the 5 V available form the USB port. Hence, all power supplies needed for a sensorized finger can be obtained from the same USB port. The PCB can be directly housed on board gripper since it is sufficiently small and light. As a consequence for each gripper a couple of fingers can be driven by a standard USB port, both from power supply and serial communication point of view. Details of the latter PCB are shown in Fig. 2. Fig. 3 shows the integration of sensorized fingers in different commercial grippers.

Algorithm 1 ROS node for data acquisition

procedure SENSORINIT
  $devices\_list \leftarrow$ get connected devices
  for $k \leftarrow 1$ to length of $devices\_list$ **do**
    $sensor\_ID \leftarrow$ ask ID of $devices\_list(k)$
    if $sensor\_ID$ is valid **then**
      add $sensor\_ID$ to $sensors\_list$
procedure SENSORSELECTION($sensors\_list$)
  print $sensors\_list$ on screen
  $selected\_sensor \leftarrow$ User selection
  open communication with $selected\_sensor$
procedure MAIN
  call $SensorInit$
  call $SensorSelection(sensors\_list)$
  set names of ROS Node and Topics
  loop:
    $raw\_data \leftarrow$ ask data to selected sensor
    if $mean\_value$ is not computed **then**
      $mean\_value \leftarrow$ mean over 50 samples
    else
      $unbiased\_data \leftarrow raw\_data - mean\_value$
      publish raw_data on the topic
      publish $unbiased\_data$ on the topic

B. ROS Nodes

In order to acquire the data captured by the tactile sensors presented in the previous section, a ROS node has been written. The pseudocode for this node, called *read_sensor_node*, is reported in Algorithm 1, where we can see three procedures. The procedure named *SensorInit* obtains the list of all the devices connected to the computer and then discards the incompatible ones. The procedure named *SensorSelection*, instead, prompts the user to select the sensor to use among those in the list and starts the communication with it. Lastly, the *Main* procedure, after calling the other two procedures, starts a loop in which, in case the node just started, it computes the mean value of the voltage signals, otherwise it publishes the raw and unbiased data on the respective ROS topics with a frequency of 500 Hz.

These unbiased voltage signals are then received by a second ROS node, in charge of analyzing them and plotting the estimated pose of the grasped wire. The pseudocode for this node, called *tactile_plotter_node*, is reported in Algorithm 2, and is composed by six procedures. The execution of the node starts with the *Main* procedure. Here, first of all, the procedure named *SystemConfiguration* is called, where the user can select the finger to use, among the ones that are publishing their values, as well as the type of regression that will be used for the estimation of the cable pose: linear or quadratic. Then, the subscriber to the topic of the selected finger is initialized. When new information is published in that topic, the *SubsCallback* procedure is called, saving the received data in a global variable. After this, an object of the class *MainWindow* is created, calling its *Constructor* procedure that initializes the graph window and establishes the refresh

Algorithm 2 ROS node for data analysis and plotting

procedure SYSTEMCONFIGURATION
  $fingers\_list \leftarrow$ get published finger topics
  $finger\_topic \leftarrow$ user selection from $fingers\_list$
  $reg\_index \leftarrow$ user selection: line or quadratic
procedure SUBSCALLBACK($finger\_topic\_msg$)
  $finger\_data \leftarrow finger\_topic\_msg$
procedure UPDATETACTILEDATA
  max_v, $min\_v \leftarrow$ get max, min $finger\_data$
  $taxels \leftarrow$ fill 5×5 matrix with $finger\_data$
  $sizes \leftarrow \frac{taxels - min\_v}{max\_v}\ max\_size$
  $rows\_V, cols\_V \leftarrow$ sum of every row and column
  if min($rows\_V$) $\geq$ min($cols\_v$) **then**
    $cent\_x, cent\_y \leftarrow$ calculate the y=f(x) centroids
    $reg\_param \leftarrow$ regre($cent\_x, cent\_y, reg\_index$)
    $line\_x, line\_y \leftarrow$ populate with reg_param
  else
    $cent\_y, cent\_x \leftarrow$ calculate the x=f(y) centroids
    $reg\_param \leftarrow$ regre($cent\_y, cent\_x, reg\_index$)
    $line\_y, line\_x \leftarrow$ populate with reg_param
class MAINWINDOW
  procedure CONSTRUCTOR
    Window and graph config and initialization
    Start $plot\_refresh\_period$ timer $\rightarrow$ 50 ms
  procedure UPDATEPLOT
    call $UpdateTactileData$
    $grasping \leftarrow$ False
    if any $taxels > grasping\_threshold$ **then**
      $grasping \leftarrow$ True
      $colors[row][col] \leftarrow$ red
    $rows, cols, sizes, colors \rightarrow$ Plot taxels
    publish reg_param and $grasping$ on topics
    if $grasping$ **then**
      $cent\_x, cent\_y \rightarrow$ Plot centroids
      $line\_x, line\_y \rightarrow$ Plot regression line
procedure MAIN
  call $SystemConfiguration$
  Initialize ROS Node, Topics and variables
  Create $MainWindow$ object
  loop:
    ROS Subscriber msg $\rightarrow$ call $SubsCallback(msg)$
    $plot\_refresh\_period \rightarrow$ call $UpdatePlot$

frequency, to automatically call its *UpdatePlot* procedure each 50ms. This procedure first calls the *UpdateTactileData* procedure to analyze the most recent tactile data and to update the information needed for plotting: taxels dots' size, centroids values and regression parameters. Once this data is updated, the *UpdatePlot* procedure determines if any object is being grasped, if the maximum voltage value is above a threshold and, in that case, the centroids and the estimated pose of the cable are plotted. Additionally, the regression parameters are published so, a node for controlling the gripper orientation can access to it, as it is done in Subsection III-B. Finally the

Main procedure enters in an infinite loop, and the node keeps listening to the subscriber and the plot updates.

III. Experiments

A. Cable Shape Detection

The WSG 50 from Weiss Robotics was the gripper utilized to mount the tactile fingers and to perform the grasping tests (left image in Fig 3). This gripper was identified to be the most suitable, as it was capable of effectively supporting the length of the fingers, along with its high resolution, applied load sensing and support for ROS. The tactile fingers are mounted on to the gripper by utilizing threaded fixtures. The cables (with external plastic jacket) of the following diameters were used as the DLO test specimen: 1.35 mm, 2.1 mm, 3.1 mm, 7.5 mm and 12.2 mm. Additionally, we also grasped two sets of multiple cables having bundle diameters 1.5 mm and 7.1 mm. The cables are grasped in the tactile pad containing the 5×5 array of taxels. The estimated pose of the grasped cable is visualized in the ROS based plotter which is a digital representation of the voltages recorded in each individual taxel.

The ROS plotter has the following components for visualizing the taxel activation and the pose of the cable. Figures 4 and 6 shows plot generation samples, wherein the circles represent the position of the taxels. The size of the circles is an indication for the magnitude of voltage generated at each individual taxel and is conditioned with the equation:

$$circle\_size = \frac{taxel\_V - min\_V}{max\_V} max\_size$$

Where, $taxel\_V$ is individual taxel voltage, min_V and max_V are the minimum and maximum taxel voltage for the entire tactile pad for the current grasp. max_size is a dimensionless number used to scale up or scale down the size and is fixed. In addition to this, the circles have two colours i.e. red and blue. The red circle indicates the taxels which have a voltage value which is higher than a defined threshold value, used to determine when an object is grasped. Whereas, the blue circle indicates voltages which are below the defined threshold voltage. In this section the performance of quadratic estimation was tested, while the linear regression is utilized in Subsection III-B for a closed loop grasping application.

Before the DLO specimen were grasped for testing, we performed empty grasps, observing a slight uneven spike in voltage levels in a localized cluster of the taxels in the lower left corner. The tests conducted with grasped cables yield accurate representation of the cable position, shape and orientation. However, the impact of the mechanical deviations or default sensor performance can be observed in the position of the line generated in the graph when grasping small cables using very small gripper closing distance. From the left images of Fig.4, you can observe that for both the top and bottom placement of the cable, the generated quadratic lines resemble with good accuracy the shape and orientation of the grasped 1.35 mm cable. However, in the middle images of Fig.4, you can observe that when the gripper closing distance is lower

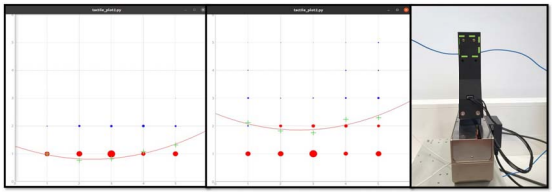

(a) Bottom cable grasp

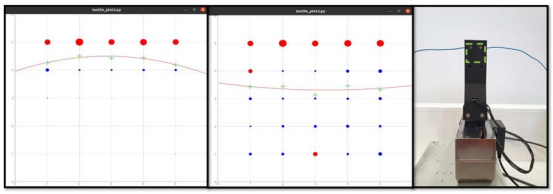

(b) Top cable grasp

Fig. 4. Comparison of the wire pose estimation using a proper gripper closing distance (left) vs using an excessive gripper closing distance (middle), at different grasping positions.

than required for a stable grasp, the tactile pad parts which are not in contact with the cable, come into contact with the opposite finger pad, increasing its voltage values and hence, slightly distorting the wire pose estimation. This effect is not very noticeable in Fig.4(a), when the cable is placed in the bottom of the pad. However, when the cable is placed in the top of the sensor area (Fig.4(b)), due to the higher empty-grasping voltage values of the lower taxels that was documented previously, the deviation in the estimated position of the cable is higher, being one of the lower row taxels even above the established threshold.

Another objective of the tactile fingers testing was to analyze the threshold value that should be established for detecting the grasping of a cable. To determine this, the maximum voltage values were observed for several gripper closing distances, when no object was grasped and when a small diameter cable (1.35 mm) was grasped, and compared. Additionally, the same experiments were repeated for multiple orientations and positions of the cable, as it was previously demonstrated that it has certain influence on the taxels maximum values. A small diameter cable was selected for this experiment because, the smaller the cable diameter, the smaller the pad deformation and therefore, the lower the taxels voltage. The results of these experiments are summarized in Fig. 5, from which some conclusions can be extracted. First of all, we can verify what was anticipated in the previous experiments, the cable detection slightly depends on its position and orientation within the tactile pad, as the voltage values are higher when the cable is placed in the bottom or in the left of the pad. We can also confirm that a 1.35 mm cable can be detected with the tactile fingers at any position, as the maximum voltages corresponding to cable grasps are always higher than the empty grasp ones, however the threshold must be defined as a function of the fingers closing distance. Additionally, this graph can explain the distortion in the cable pose estimation observed in Fig. 4, as for cable grasped with the top of the finger pad, the voltage of the taxels in contact with the cable

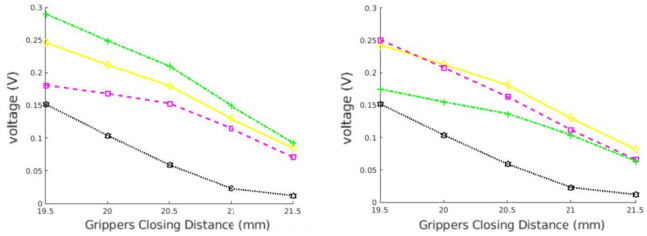

(a) Horizontal empty (black), bottom (green), middle (yellow) and top (pink) grasps

(b) Vertical empty (black), left (yellow), middle (pink) and right (green) grasps

Fig. 5. Maximum taxel voltage values at different gripper closing distances, when doing an empty grasp and a 1.35 mm cable grasp at different horizontal (a) and vertical (b) positions.

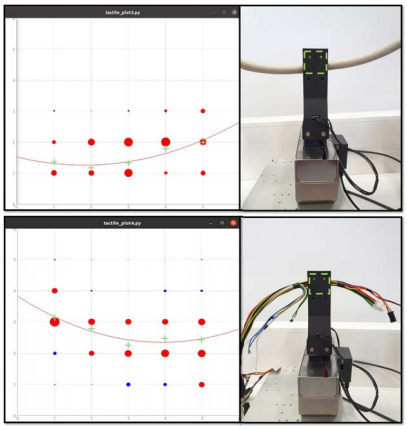

Fig. 6. 12.2 mm cable (top) and 7.1 mm harness (bottom) grasps and pose estimation

becomes very similar to the empty grasp voltages when the gripper closing distance is very small, so its weight in the centroids calculation is very high.

Finally, some experiments were performed to test the pose estimation of cables with different diameters, ranging from 1.35 to 12.2 mm, and a branch of cables taped together. Five single cables with diameters of 1.35, 2.1, 3.1, 7.5 and 12.2 mm, as well as a group of eleven cables taped together, with an equivalent diameter of approximately 7.1 mm, were grasped, and the taxels activation and the pose reconstruction at different gripper closing distances were analyzed. For these experiments the grasping threshold was manually set as 0.14V. As can be observed in Fig. 6, the pose estimation for the 12.2mm cable is very accurate but it was not as good for the wire harness, because its shape became flatter when we press it, however the general orientation of the harness can be obtained. From these experiments it was also observed that the maximum voltage values (at a gripper closing distance enough to provide a stable grasp) increases with the cable size. Thus, the threshold function should also depend on the cable diameter if we want to detect stable grasps.

B. Grasping Pose Correction

In this experiments, the tactile sensor mounted on the Schunk PG70 gripper is exploited to improve the capability

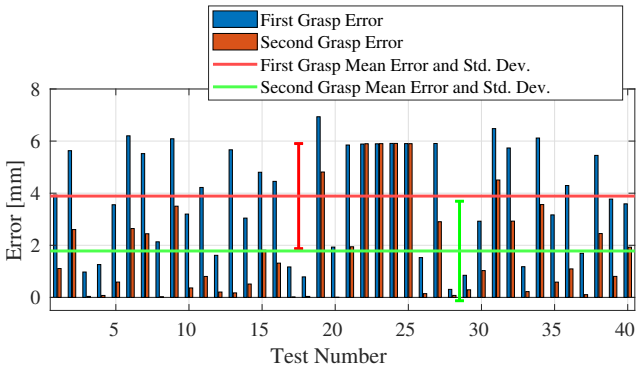

Fig. 7. Comparison of the position error during the first and the second grasp.

of the robot of grasping a cable with diameter of 2.5 mm with the right pose in terms of position and orientation, e.g. with respect to the center of the sensor and a direction normal to the finger plane. The cable is suspended between two supports in a known position. However, the way how the cable is grasped is inferred by the deformability of the cable itself, and in particular by its initial shape and pose. Therefore, in case it is not possible to detect the shape of the cable before executing the grasp, e.g. by means of a vision system, such as in case the visibility of the grasp location is occluded, the only way to detect if the cable is correctly aligned with the gripper fingers is by means a tactile sensor.

1) Adjusting Grasp Vertical Offset: Given a predefined cable grasp configuration, a random-generated value in the range ± 12.5 mm, which correspond to the size of the tactile sensor, is added to the grasping pose along the z axis to simulate the uncertainties in the cable location. The resulting grasp pose is then adopted by the robot as first grasp trial. Once the finger are closed over the cable, the position and orientation of the wire with respect to the tactile reference frame is estimated with a first order model as a straight line

$$y = mx + c$$

where the parameter c represent the distance between the cable and the center of the sensor area while m is the angular coefficient. Thereafter, the cable is released, the value c is then used to correct the the gripper pose along the z axis and perform the second grasp in order to achieve $c^* = 0$.

The plot in Fig. 7 shows the value of the parameter c during the first and the second grasp during 40 trials. It is possible to see that the correction of the gripper pose based on the information provided by the tactile sensor can reduce the cable alignment error with respect to the center of the sensor. In particular, the mean error and standard deviation at the first are 3.9 mm and 2.0 mm respectively, while they reduce to 1.8 mm and 1.9 mm respectively at the second grasp. The error at the second grasp is given by the fact that since the cable is not rigid, the interaction with the gripper and can slightly change the actual cable position between the two grasps.

2) Adjusting Grasp Orientation: In this scenario, the rotation of the cable with respect to the sensor surface is also

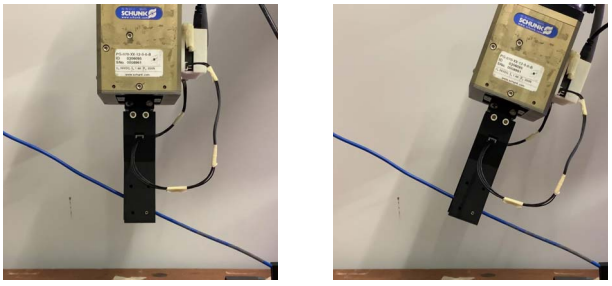

(a) First Grasp (b) Second Grasp

Fig. 8. Cable regrasping sequence: once the first grasp is achieved, the tactile map is used to estimate the position and orientation of the cable and adjust the final orientation and position for the second grasp.

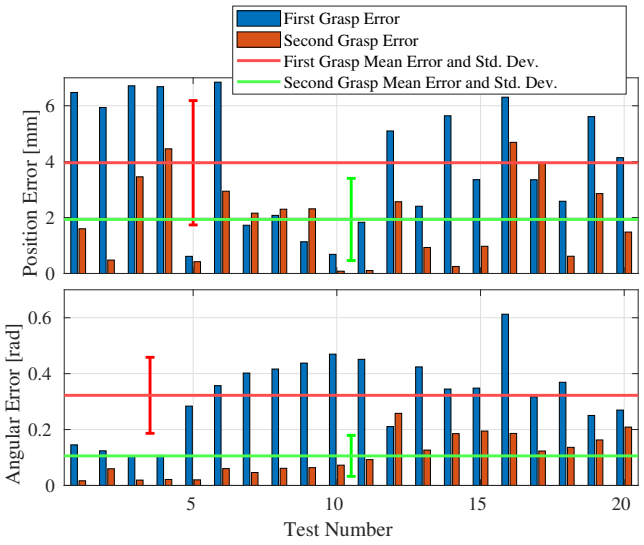

Fig. 9. Experimental results obtained with uncertainties in both displacement and orientation.

taken into account. Then, the orientation estimated through the tactile sensor enable to compensate the error during the second grasp in order to achieve both $c^* = 0$ and $m^* = 0$. The sequence of grasps is reported in Fig. 8. As reported in Fig. 9 showing the results of 20 trials, the gripper is able to address uncertainties in both displacement and orientation thank to the tactile data map. The mean position error and standard deviation at the first are $4.0\,$mm and $2.2\,$mm respectively, while they reduce to $1.9\,$mm and $1.5\,$mm respectively at the second grasp, so comparable with the previous results. About the angular error and standard deviation, they are $0.32\,$rad and $0.14\,$rad respectively during the first grasp, while they reduce to $0.11\,$rad and $0.07\,$rad respectively at the second grasp.

IV. Conclusions And Future Directions

Manipulation of deformable materials is a challenging task, where perception plays a key role for the estimation of the object's shape and pose. In this paper a perception system, consisting on a pair of tactile fingers, has been integrated with three different commercial grippers and two ROS-based nodes for the acquisition, analysis and visualization of the tactile data have been developed and tested. The performance of the tactile fingers and the ROS plotter show promising results on to the cable orientation and shape estimation. In fact, thanks to the tactile sensors data, it has been shown how it is possible to reduce the position error below $2\,$mm and the angular error below 6 degrees after regrasp.

However, certain aspects can be improved and updated to increase overall usability and to cover all the application requirements. A possible means to improve the accuracy of the grasp detection would be to integrate the sensor outputs for both fingers, optimizing the quadratic line by taking the mean of the corresponding taxel voltage values of each finger.

Another step forward could be to enable the automatic diameter detection of the cable by utilizing neural network techniques, thereby automating the determination of threshold voltage values. This enables the detection of cables with varying physical dimensions during a single operation cycle.

Finally, one of the major challenges in the grasping operation is the handling of multiple cables. From the experiments, and due to the limited physical characteristics of the gripper and the tactile sensor, detecting multiple cables when they are not taped together, requires the introduction of additional sensing techniques. This could be addressed by exploiting vision systems for detecting shape and the number information.

References

[1] M. Bergerman, J. Billingsley, J. Reid, and E. Van Henten, "Robotics in agriculture and forestry," in *Springer Handbook of Robotics*, 2016, pp. 1463–1492.

[2] T. L. Mitzner, T. L. Chen, C. C. Kemp, and W. A. Rogers, "Identifying the potential for robotics to assist older adults in different living environments," *Int. journal of social robotics*, vol. 6, no. 2, pp. 213–227, 2014.

[3] P. Y. Chua, T. Ilschner, and D. G. Caldwell, "Robotic manipulation of food products–a review," *Industrial Robot: An Int. Journal*, 2003.

[4] H. Tanner, K. Kyriakopoulos, and N. Krikelis, "Advanced agricultural robots: kinematics and dynamics of multiple mobile manipulators handling non-rigid material," *Computers and electronics in agriculture*, vol. 31, no. 1, pp. 91–105, 2001.

[5] X. Jiang, K.-m. Koo, K. Kikuchi, A. Konno, and M. Uchiyama, "Robotized assembly of a wire harness in a car production line," *Advanced Robotics*, vol. 25, no. 3-4, pp. 473–489, 2011.

[6] D. De Gregorio, R. Zanella, G. Palli, S. Pirozzi, and C. Melchiorri, "Integration of robotic vision and tactile sensing for wire-terminal insertion tasks," *IEEE Tran. on Automation Science and Engineering*, vol. 16, no. 2, pp. 585–598, 2018.

[7] G. Palli, S. Pirozzi, M. Indovini, D. De Gregorio, R. Zanella, and C. Melchiorri, "Automatized switchgear wiring: An outline of the WIRES experiment results," in *Advances in Robotics Research: From Lab to Market*. Springer, 2020, pp. 107–123.

[8] J. Sanchez, J.-A. Corrales, B.-C. Bouzgarrou, and Y. Mezouar, "Robotic manipulation and sensing of deformable objects in domestic and industrial applications: a survey," *The Int. Journal of Robotics Research*, vol. 37, no. 7, pp. 688–716, 2018.

[9] M. Costanzo, S. Stelter, C. Natale, S. Pirozzi, G. Bartels, A. Maldonado, and M. Beetz, "Manipulation planning and control for shelf replenishment," *IEEE Robotics and Automation Letters*, vol. 5, no. 2, pp. 1595–1601, 2020.

[10] D. De Gregorio, G. Palli, and L. Di Stefano, "Let's take a walk on superpixels graphs: Deformable linear objects segmentation and model estimation," in *Asian Conference on Computer Vision*. Springer, 2018, pp. 662–677.

[11] S. Pirozzi and C. Natale, "Tactile-based manipulation of wires for switchgear assembly," *IEEE/ASME Tran. on Mechatronics*, vol. 23, no. 6, pp. 2650–2661, 2018.

[12] G. De Maria, C. Natale, and S. Pirozzi, "Force/tactile sensor for robotic applications," *Sensors Actuators A: Physical*, vol. 175, pp. 60–72, 2012.